

**Development of a displacement sensor for the CERN-LHC superconducting cryodipoles**

Daniele Inaudi - SMARTEC SA, CH-9616 Grancia, Switzerland  
Branko Glisic, Sirine Fakra - EPFL, CH-1015 Lausanne, Switzerland  
Jacques Billan, Juan Garcia Perez, Stefano Redaelli, Walter Scandale - CERN, CH-1211  
Geneva 23, Switzerland

**Abstract**

One of the main challenges of the Large Hadron Collider (LHC), the particle accelerator under construction at CERN (the European Organization for Nuclear Research) in Geneva, resides in the design and production of the superconducting dipoles used to steer the particles around a 27 km underground tunnel. These so-called cryodipoles are composed of an evacuated cryostat and a cold mass, that contains the particle tubes and the superconducting dipole magnet and is cooled by superfluid Helium at 1.9 K. The particle beam must be centred within the dipole magnetic field with a sub-millimetre accuracy, this requires in turn that the relative displacements between the cryostat and the cold mass must be monitored with accuracy.

Because of the extreme environmental conditions (the displacement measurements must be made in vacuum and between two points at a temperature difference of about 300 degrees) no adequate existing monitoring system was found for this application. It was therefore decided to develop an optical sensor suitable for this application.

This contribution describes the development of this novel sensor and the first measurements performed on the LHC cryodipoles.

*Paper submitted to Measurement Science and Technology*

Administrative Secretariat  
LHC Division  
CERN  
CH-1211 Geneva 23  
Switzerland

Geneva, 2 February 2001

# 1 Introduction

The Large Hadron Collider (LHC) is a hadron circular collider under construction at the European Organization for the Nuclear Research (CERN) [1]. The LHC will be installed in a 27 km long underground tunnel in the area near to Geneva and will accelerate two counter-rotating colliding proton beams, each at a 7 TeV energy. This project is aimed at studying the interactions of the basic constituents of the matter at the multi-TeV energy level; this is supposed to enlighten our knowledge on Higgs particles and on the theory of Supersymmetry. High magnetic fields are required to bend the proton beams to the desired curvature radius; they will be provided by 1232 *dipole magnets*, which will generate a 8.3 Tesla field. Superconducting technology makes this possible.

The 1232 superconducting main dipole magnets will be distributed over eight arcs and will operate in a superfluid helium bath at 1.9 K. The cold masses of 15 m length will be made up of coils of superconducting niobium-titanium alloy cable maintained in shape and place by austenitic steel collars. These in turn are contained within a magnetic circuit consisting of low-carbon steel laminations with non-magnetic steel end-laminations. A welded austenitic stainless-steel shrinking cylinder, made up of two welded half cylinders (shells), surrounds the whole and also acts as the liquid helium vessel. A cross section of the LHC main dipole is given in figure 1.

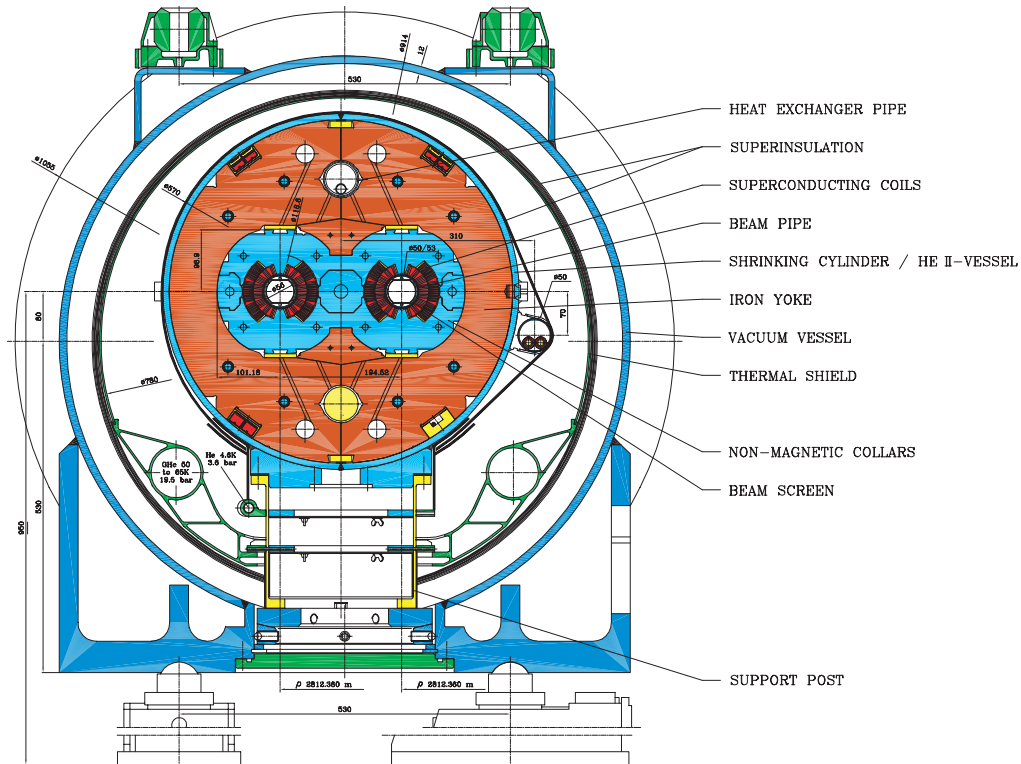


Figure 1: Cross section of the LHC cryodipole.

Each dipole cold mass is enclosed in a cryostat, that consists of three supports for the cold mass, a radiation screen and a thermal screen both equipped with multi-layer super-insulation, and a vacuum vessel. Each dipole contains two stainless steel beam pipes inserted in the coil apertures where the two counter-rotating beams circulate. The dipole assembled into the cryostat forms the cryodipole magnet, which is around 35 tonnes heavy.

Dipole and quadrupole magnets, with a number of other correcting and auxiliary

magnets, will be installed in the LHC underground tunnel to properly guide the beam particles on their orbit, according to a precise focusing scheme called lattice. To ensure the LHC performances, very tight tolerances on the magnet alignment, of the order of some tenths of millimetres, are imposed. These tolerances are difficult to be achieved, in particular for the very long LHC dipoles. One of the greatest source of uncertainty for the alignment of the superconducting magnets is that each magnet is installed in a cryostat, that completely hides it to installation and survey teams. As a consequence one has to refer the cold mass position to some external references on the cryostat when the magnet is installed in the vacuum vessel. In order to correlate the cold mass position to the external references, it would be worth to precisely monitor the displacements of the cold mass with respect to the cryostat, during the different steps needed to install and align the magnets in their final position in the LHC tunnel.

The installation in the cryostat is performed at room temperature and there are two main possible sources of dipole displacements:

- deformations induced by temperature variations and by the temperature gradients during the magnet cool down;
- displacements during the transportation of the magnet in the tunnel.

In addition, the magnets can also undergo movements in case of transition to the normal conducting state and during energization, but these effects should be less critical since they are expected to be smaller than the previous ones.

The effects of the temperature variation on the dipole are quite difficult to be foreseen. Indeed, the dipole geometry is very complex: it is an inhomogeneous cylinder, 15 m-long, bent horizontally by about 5 mrad, and made of laminations of different materials (basically, iron and austenitic steel). Since the Helium refrigerating the cold mass is injected from one side and flows towards the other side through the heat exchanger pipe, during the cool down longitudinal temperature differences up to 60 degrees or more arise between the two ends.

Each dipole has a set of short corrector magnets (sextupole, octupole and decapole) located at the ends to correct in a quasi-local manner systematic field errors. Such correctors must be aligned to the dipole axis with a tolerance in the transversal direction of 0.3 mm [2]. In addition, too large dipole displacements, even those induced by thermal gradients during cool down, can be detrimental for the interconnections between consecutive magnets installed along the beam path. In this case, the relative displacements of the dipole ends should be smaller than 1 mm.

In this paper, we present an innovative system developed in a collaboration between CERN (Geneva, CH), IMAC-EPFL (Lausanne, CH) and SMARTEC SA (Lugano, CH), to monitor cold mass movements relative to the cryostat. The detector is inspired from a system used for monitoring the deformation of civil-engineering structures [3, 4]. The standard sensor, with two optical fibres, is not suitable for measuring the dipole displacements relative to the cryostat during cool down, since the cold mass shrinks longitudinally by about 40 mm, due to thermal contraction. This shrinkage prevents us to measure transverse displacements with an optical fibre installed between cold mass and cryostat. Therefore, it was decided to use a light beam propagating in the free space between an optical head, welded on the cryostat inner wall, and a mirror, welded on the outer part of the cold mass. We present here the early measurements performed on prototype dipoles.

In section 2 we describe the functioning principles of the selected monitoring technique. In section 3 we present the criteria inspiring the new sensor design that we developed. In section 4 we present a selection of our experimental results and finally in section 5

we draw some conclusions.

## 2 Selected monitoring technique

The measurement system that was used for the LHC cryodipole is an evolution of a deformation monitoring system originally developed by IMAC-EPFL and SMARTEC SA to monitor deformations of civil-engineering structures, called SOFO (French acronym of *Surveillance d'Ouvrage par Fibres Optiques*, i.e. Monitoring of Structures by Optical Fibres) [5, 6, 7], but it also finds applications in other domains [9]. It is based on a low-coherence double interferometre in tandem configuration, used to measure the optical path difference between two fibres, called measurement and reference fibres, respectively [3, 4, 8]. In our case, as explained in section 3, we do not measure a fibre deformation, but the distance between a mirror welded on the cold mass and an optical head fixed on the cryostat.

A scheme of the original SOFO system is shown in figure 2 [3]. The laser source is provided by a Light-Emitting Diode (LED), working at  $1.3\ \mu\text{m}$  with a coherence length of  $30\ \mu\text{m}$ ; the radiation is launched into a single-mode standard telecom fibre and then

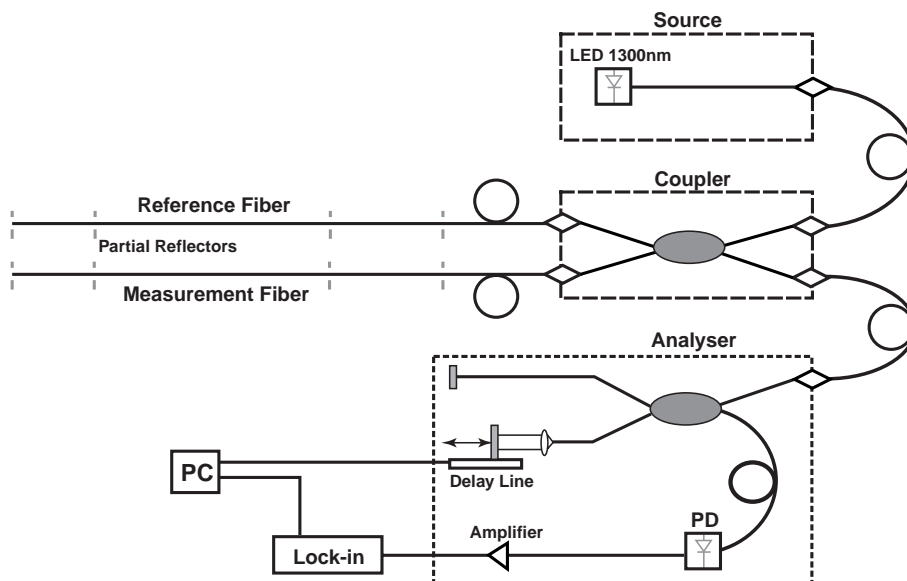


Figure 2: Scheme of the interferometers in tandem configuration used in our measurement system [3].

directed towards the two fibres by means of a directional coupler. The two beams are reflected back to the coupler by mirrors placed at the end of the two fibres, they are recombined with a relative delay due to the length difference between the two fibres and eventually they are directed through a second coupler to a reference interferometer. This is a Michelson-type interferometer, with one of the arms ended by a mobile mirror mounted on a micrometric displacement table with a resolution of  $1\ \mu\text{m}$  and an operating range of 80 mm: it allows the introduction of an exactly known path difference between the two arms. When such a difference corresponds to the one induced by different length variations between the reference and measurement fibres (within the coherence length of the source), interference fringes appear, that are registered with a photo-diode. The measurement of the distance between the interference peaks allows to obtain the amount of the deformation of the measurement fibre.

Table 1: Specifications of the SOFO system [10].

Parameter	SOFO characteristics
Measurement basis	20 cm to 10 m for standard sensors
Resolution	0.002 mm
Precision	Better than 0.2% of the measured deformation
Dynamic range of the sensors	1% elongation, 0.5% shortening for standard sensors
Dynamic range of the reading unit	Up to 80 mm in elongation and shortening
Cable length (information carrier)	Up to 5 km
Temperature sensitivity	Insensitive, self-compensated sensors
Long-term stability	Good, drift not observable over at least five years
Acquisition time	Less than 15 seconds
Automatic and remote monitoring	Possible permanent, automatic and remote static monitoring
Environmental influences	Insensitive to humidity, corrosion, vibration, electro-magnetic fields and temperature

All these components are implemented in the SOFO technology, which consists of three main elements: a reading unit (containing the LED, the low-coherence Michelson interferometer with a mobile scanning mirror, the optical components and an internal personal computer), the fibre optic sensor and an acquisition and management software [6]. The main characteristics and performances of the SOFO system are listed in table 1.

### 3 Displacement sensor design

#### 3.1 Design criteria

The use of the standard fibre optic sensor to measure LHC cold mass displacements is not possible, mainly due to the large longitudinal contraction of the cold mass during the cool down ( $\sim 40$  mm), which prevents to attach a fibre between the cold mass and the vacuum vessel inner wall, but also because of installation difficulties and the thermal bridge it creates.

The solution to this problem was obtained by developing a new displacement sensor, in which the measurement fibre is substituted by a light beam propagating in vacuum between the inner wall of the cryostat (where an optical head is attached, see section 3.2) and the outer part of the cold mass (where a special mirror is welded). This provides measurements of relative displacements between cold mass and cryostat. Optical fibres are used as reference path in the optical head and to bring the light in and out of the vacuum tube.

The extreme environmental conditions (1.9 K temperature and vacuum) and the geometry have imposed several restrictions to the displacement sensor design.

The cold mass mirror is subjected to temperatures as low as 1.9 K and must survive undamaged during the cool down. Tests showed that a high quality mirror with gold coating could survive these extreme conditions without damages (see section 3.5). The dimensions of the mirror are 50 mm $\times$ 50 mm $\times$ 10 mm.

The optical head, installed on the interior of the vacuum vessel, has to be connected with the reading unit, which is at the exterior, with optical fibres; a special vacuum feedthrough has been conceived for this purpose (see section 3.3). The feedthroughs have to function in vacuum without significant outgassing.

During cooling and operation, the cold mass experiences small unwanted horizontal

and vertical rotations. As a result, the cold mass mirror is subjected to tilt. A tilt can also be introduced by a poor alignment of the mirror with respect to the incoming light beam. The estimated tilt of the cold mass mirror is less than 1 mrad. Tilt influence on the measurement is restricted using a double pass delay line (see section 3.4).

The working distance of the sensor is approximately 100 mm or 200 mm for horizontal and vertical heads, respectively (see section 4.1); combined with a possible tilt of the cold mass mirror, such large working distances can decrease significantly the intensity of the reflected beam, which is indispensable for good measurements.

### 3.2 Concept of Displacement Sensor

A schematic representation and photo of the optical head without its cover as well as the principle of functioning of the displacement sensor are presented in figure 3. The

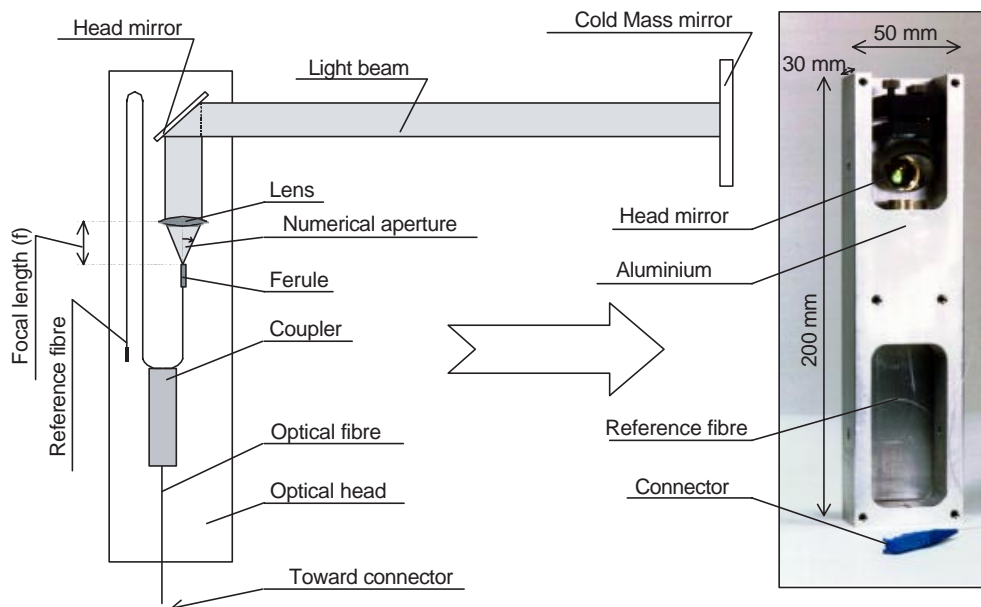


Figure 3: Scheme, photo and principle of functioning of displacement sensor.

optical head has to be inserted between the thermal shield and the vacuum vessel; the small distance between them limits its transversal dimension to 30 mm. The optical head consists of a coupler, reference fibre, ferrule, lens and the head-mirror, as shown in figure 3; its dimensions are 30 mm×50 mm×200 mm. All parts of the optical head are protected by an aluminium armour. The optical head, including the reference fibre, is thermalised with the vacuum vessel, so it works almost at constant room temperature. The optical path and the reference fibre have about the same optical length and constitute a Michelson interferometer. This interferometer is demodulated using the SOFO reading unit.

### 3.3 Design of the feedthrough

The feedthrough is made of an FCPC (standing for Fibre Connector Physical Contact) connector and the corresponding mating adapter glued into an opening in the steel feed. The gluing is realised using a special vacuum-resistant epoxy resin (Torr Seal by Varian). This resin fills up all gaps around the connector and the mating adapter. A schematic representation and a picture of the feedthrough prototype are presented in figure 4.

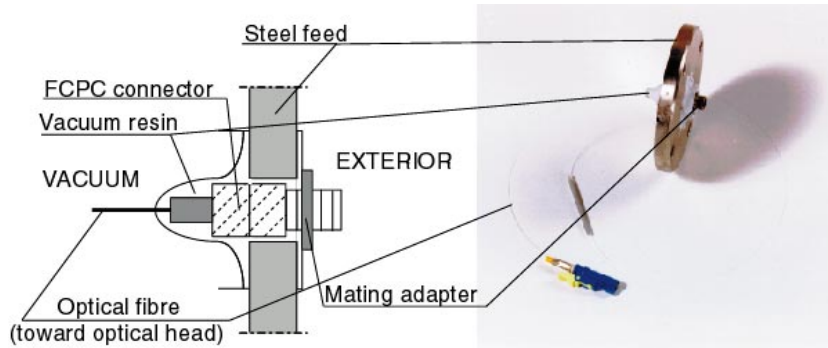


Figure 4: Scheme and photo of feedthrough prototype.

### 3.4 Functional principle - double pass delay line

The sensor functions as follows (see figure 5): the broadband light coming from the reading unit is split by the coupler. One path goes into the reference fibre while the second leaves the fibre through a metallic ferrule which is collimated by the lens and pointed by the head mirror towards the cold mass mirror. The light reflects off the cold mass mirror, goes back to the lens and is collimated on a point on the ferrule, close to the optical fibre end, but not on it. The reflected light travels back to the cold mass and is finally reflected and collimated back in the optical fibre. Since the fibre core and the reflection point on the ferrule are conjugated points with respect to the lens-mirror system, the light is always reflected back to the fibre core after two passes, independently from the mirror tilt. The

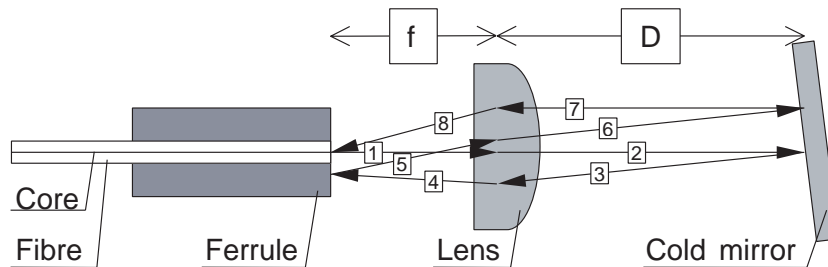


Figure 5: Double pass delay line.  $f$  is the focal length and  $D$  is the distance to be measured. The trajectory of the light is indicated by progressive numbers.

intensity of the re-coupled light will depend on the aperture-matching and will be reduced with increasing rotation of the mirror [8, 10]. This set-up ensures a back-coupling with high tolerance on the cold mass mirror rotations and independence on its longitudinal translations. In general, a longer focal length of the lens will improve the angle range, but increases the head and beam size.

### 3.5 Laboratory tests

The following preliminary tests [9, 10] were carried out in order to qualify the sensor before installation in the cryodipole prototypes:

- Back coupling efficiency of the sensor
- Resistance of the cold mass mirror in low temperature conditions
- Behaviour of the materials constituting the prototype under vacuum
- Influence of vacuum to the optical head - cold mass mirror alignment
- Acceptable tilt range

The back coupling efficiency of the sensor represents the intensity of light that comes back into the reading unit after passing through the double pass delay line. The intensity of the back light depends on the distance between the optical head and the cold mass mirror, the angle between the incoming light beam and the axis perpendicular to the cold mass mirror (tilt of the mirror), the lens focal length and the numerical aperture of the fibre. The aim of this test was to examine the functional principle and to determine the properties of the optical components of the sensor allowing good measurements for the foreseen working distance (150 mm) and tilt (1 mrad). The back coupling efficiency was tested using a set-up consisting of an optical head and a cold mass mirror, both mounted on displacement table. The distance between the optical head and the cold mass mirror is controlled using a micrometer. The ferrule with a numerical aperture of 0.12 and the lens with a focal length of 25.4 mm allow a sufficient back coupling efficiency at the working distance.

The resistance of the cold mass mirror in low temperature conditions was tested at three different temperatures, at 77 K using liquid nitrogen, at 20 K using a refrigerator and at 4.2 K using liquid helium. The first two tests were carried out at IMAC and the third one at CERN. These tests showed that the selected mirror can survive without noticeable damage to the cool-down.

The behaviour under vacuum of the materials constituting the prototype was tested at IMAC using a small vacuum chamber, using the prototype head and mirror. Two phenomena were tested: the outgassing of all components and the leaking of the feedthrough. At first, only the optical head and the cold mass mirror were placed into the vacuum chamber and the vacuum was established. Afterwards, the feedthrough was installed and the experience was repeated. No outgassing was observed during the first test. The pumping set-up did not take approximately the same time to reach the final pressure ( $2 \cdot 10^{-6}$  mbar) in the vacuum chamber as for the empty chamber. On the other hand, during the second test a small outgassing was observed: a longer stagnation at a  $10^{-5}$  mbar pressure was noticed. The ultimate pressure was reached in 550 minutes instead of 300 minutes. This outgassing was small enough to be neglected in the LHC conditions (15 m long vessel). Moreover, the feedthrough was not leaking, since the pressure was continuing to decrease even in presence of the released gas.

The influence of the vacuum in the alignment between optical head and cold mass mirror was tested using the same set-up as in the previous test. The cold mass mirror was aligned at atmospheric pressure and fixed at a working distance of approximately 140 mm. The pressure was firstly decreased to  $5.4 \cdot 10^{-5}$  mbar and afterwards increased to the initial atmospheric pressure. Measurements were repeated during both phases of the test and no effect on the head or mirror alignment was observed. A change of approximately  $80 \mu\text{m}$  was seen in the mirror-to-head distance in vacuum. This apparent shift is in fact related to the different speed of light in air and in vacuum. An appropriate correcting coefficient was found for the reading unit.

The cold mass mirror may be exposed to horizontal and vertical tilts. If the tilt exceeds a certain value, the back-coupling efficiency might become insufficient to carry out a measurement. The acceptable tilt range was determined by simulating a mirror tilt with a rotation stage.

The cold mass mirror was attached to a support whose horizontal and vertical tilts were controllable and measurable. The tilt was imposed to the mirror and measurements were carried out with the optical head. An example of results for horizontal tilt is shown in figure 6. Displacements are found as a function of the tilt angle due to a misalignment



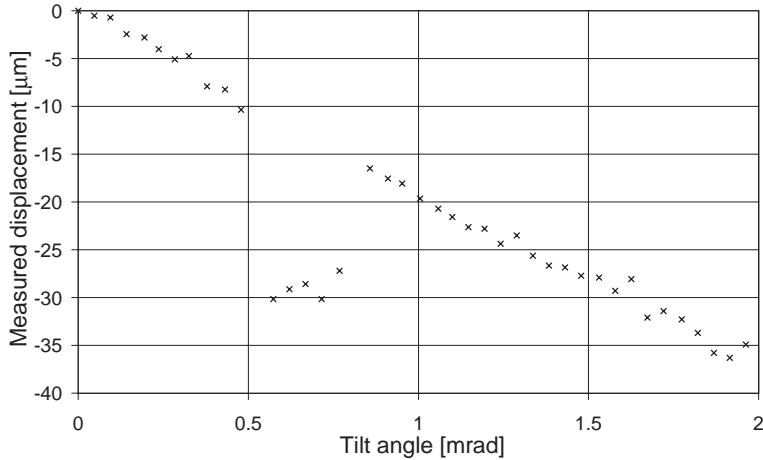


Figure 6: Horizontal measurements as a function of the mirror tilt. The variation of the measured distance is induced by a misalignment between laser beam and the centre of rotation of the mirror.

between the laser beam and the rotation centre. This is caused by eccentricity between the light beam and axis of rotation of the mirror. The tilt that allows return of the light to the optical head can be easily found.

The usable measurement area is divided in two zones with a blind area in-between. This interruption is expected and corresponds to the light beam returning directly into the fibre cladding after a single round trip (see figure 5). Therefore the area that is considered as exploitable for measurement begins after the interruption and finishes when the signal fades. This area cover a range of 1.12 mrad for horizontal and 1.55 mrad for vertical tilt. These values are higher than the maximal tilt that can be tolerated in the cryodipole. The sensors should therefore cover the whole utilisation spectrum without the need of realignments.

## 4 Experimental results

### 4.1 Installation

Our system measures absolute variations of the distance between the mirrors, welded on the cold mass, and the optical heads, fixed on the cryostat. Displacements of the dipole relative to the cryostat in the plane perpendicular to the magnet longitudinal axis can be monitored by measuring distances between cold mass and cryostat inner wall in three points. Three optical heads are installed at around 500 mm from the magnet ends, as shown in figure 7: two of them are placed along a horizontal diameter of the cold mass and allow measuring diameter variations (given by the sum of measured distance changes) and horizontal centre displacements (given by the semi-difference of the measured distance changes). The third head measures the vertical distance between the lower part of the cold mass and the cryostat: this provides a measurement of vertical displacements of the magnet centre, once the variation of the dipole radius is subtracted.

This experimental set-up enable us to measure cold mass displacements relative to the cryostat and diameter variations in different situations, such as transportation, thermal cycles, magnet energization and quenches [11].

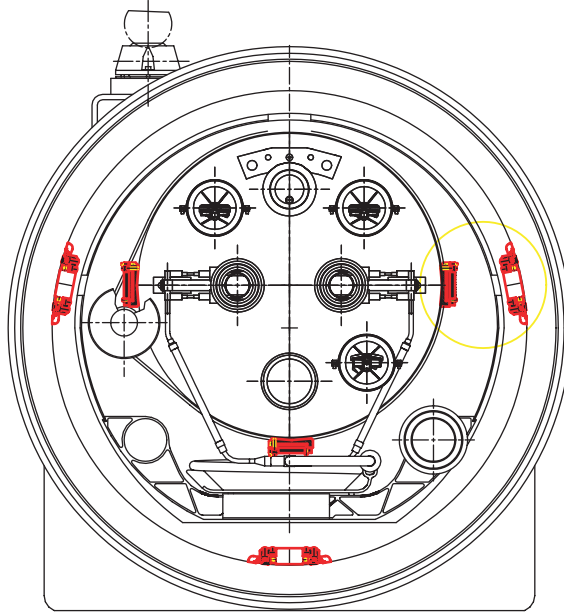


Figure 7: Installation of the optical heads on the cryostat and of the mirrors on the cold mass. They are longitudinally located at around 500 mm from magnet ends.

#### 4.2 Dipole displacement during transportation

After cryostating, the dipoles have to be installed in the underground tunnel: one is interested in monitoring displacements during transportation.

Examples of vertical and horizontal displacements of the dipole relative to the cryostat during the transportation by truck between two CERN buildings are given in figures 8 and 9, respectively. Measurements are taken about every minute. We indicate the various

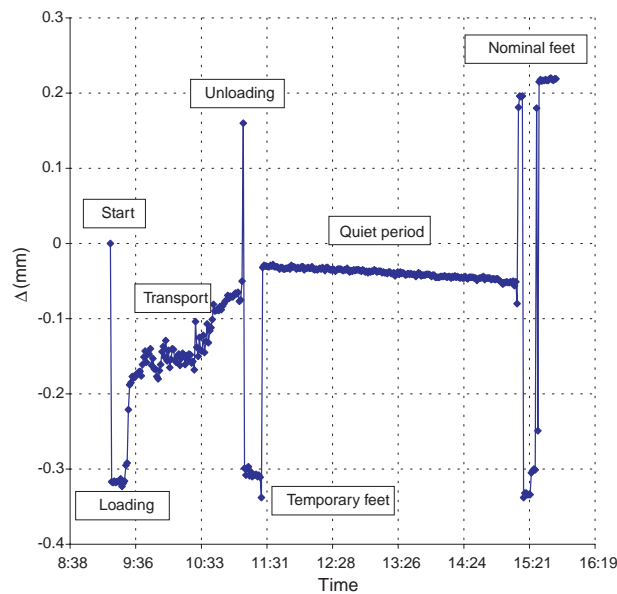


Figure 8: Vertical displacements of the dipole prototype MBP2O2 during transportation.

operations performed, namely the loading on the truck, the transportation, the unloading from the truck, the installation on temporary feet, a quiet period (during which the dipole was sitting on the floor) and the final installation on the nominal feet. The largest

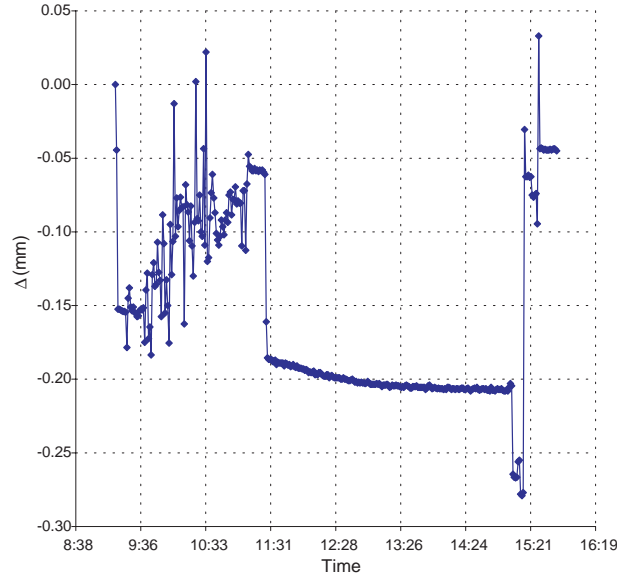


Figure 9: Horizontal displacements of the dipole prototype MBP2O2 during transportation.

displacement is observed when the magnet is lifted with a crane to be loaded and unloaded from the truck. Maximum displacements up to around 0.5 mm and 0.3 mm were measured, in vertical and horizontal directions, respectively. On the other hand, the final offsets between starting and final positions (with the nominal feet configuration) are smaller, i.e. around 0.2 and 0.05 mm, respectively. The band-width of the system is insufficient to follow the fast cold mass vibrations during the transportation and the measured displacements might underestimate the real maximum movements.

### 4.3 Deformations during thermal cycles

One would like to monitor dipole displacements during cool down to check whether the alignment at room temperature is maintained at 1.9 K. We measured cold mass displacements relative to the cryostat and diameter variations during several thermal cycles performed on the dipole prototypes.

A typical plot of dipole displacements and diameter variations as a function of the time during a standard thermal cycle is given in figure 10: starting from the 1.9 K operational temperature, the cold mass is warmed up and then cooled down again at 1.9 K. Diameter variations, centre displacements (both in vertical and horizontal directions) and the temperature on the considered magnet end are given as a function of time. Notice that the vertical head was not available for the whole temperature range, since unexpected movements of the lower part of thermal screen (see figure 1) eventually cut the light path to the mirror.

During the transition from room temperature to 1.9 K, the cold mass diameter shrinks by about 1.3 mm. An example of the measured variations as a function of the temperature is given in figure 11, for both ends of one prototype (data refer to a warm up cycle). The measured value is consistent with the expected one, assuming the known thermal coefficients for iron and stainless steel.

Centre displacements as a function of the temperature measured on both ends of a prototype are shown in figure 12. A similar pattern is found in the two cases, but the two shifts have rather different values. Final offsets with respect to the position at room

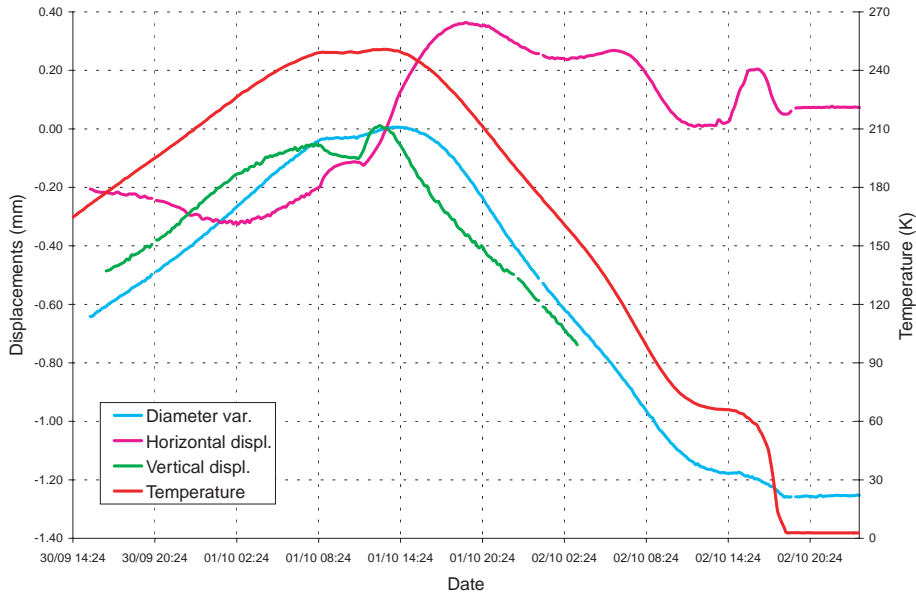


Figure 10: Horizontal and vertical displacements of the centre of the cold mass and diameter variations as a function of the time during a thermal cycle performed on the MBP2A2 prototype between September 30 and October 2, 2000. The temperature on the considered side is also given.

temperature are up to 0.3 mm, i.e. of the order of tolerances on corrector alignment. One should wait for more statistics to see whether such a feature is systematic and possibly try to compensate for it. During the whole thermal cycle, larger displacements of the dipole end centre are found, up to more than 2 mm. This is a potential problem for the interconnections between two consecutive magnets.

Vertical displacements up to more than 1 mm have been observed in the temperature range where the acquisition system has been working, i.e. from room temperature to around 150 K. They are mainly induced by the contraction of the dipole feet. Further variations are expected at least down to 100 K.

#### 4.4 Deformations during energization

During the magnet energization, electromagnetic forces arise in the coil, which depend on the square of the exciting current. At the nominal current, in the straight part of the dipoles, there are outwards horizontal forces of the order of 3 MN/m. Moreover, in the dipole ends, forces with a longitudinal component of the order of 0.5 MN also arise [1].

We measured small dipole deformations when the current is ramped up to the nominal value of 11.75 kA. The horizontal diameter increases by around  $60 \mu\text{m}$ , according to the mentioned quadratic dependence on the exciting current  $I$  (see figure 13). The order of magnitude of such a variation is in agreement with an estimation based on mechanical properties of the dipole. Also the centre of the cold mass end moves, up to around  $80 \mu\text{m}$ , and it features a quadratic dependence on  $I$  as well.

#### 4.5 Movements after a quench

A *quench* is a sudden transition of a superconductor to the normal-conducting state. At the operational field, a current of 11.75 kA flows in the cables and an energy of around

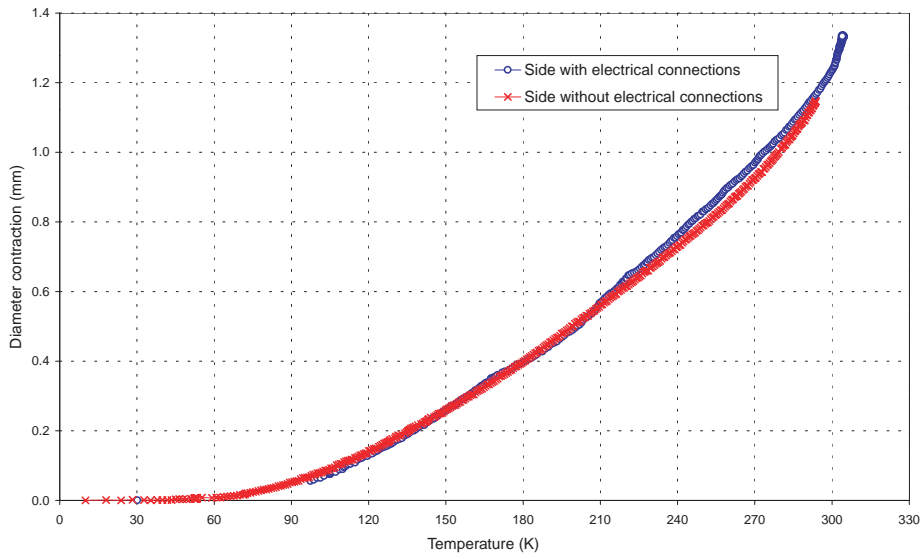


Figure 11: Diameter variation as a function of the temperature for the two sides of the MBP2A2 prototype. Zero diameter refers to its value at 1.9 K.

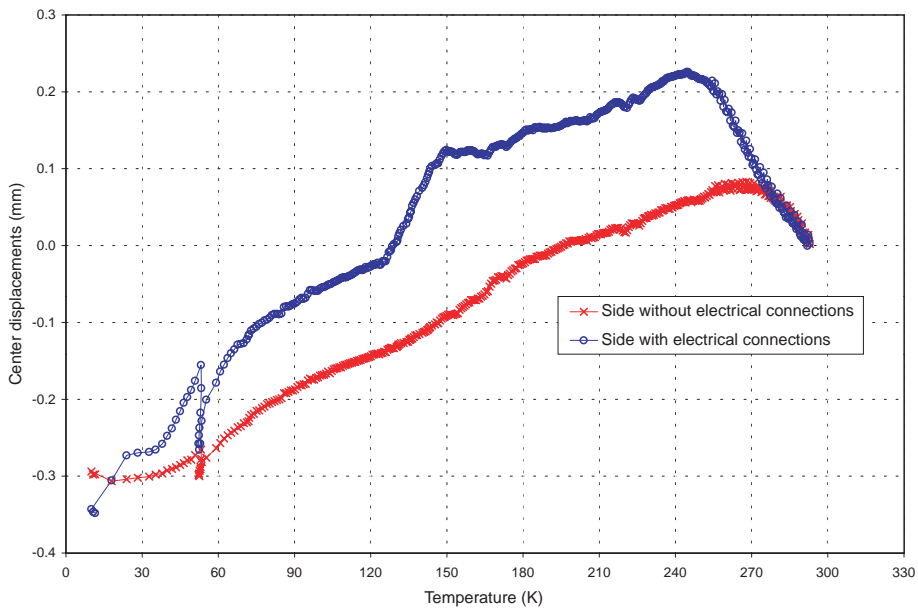


Figure 12: Centre displacement as a function of the temperature for the two sides of the dipole prototype MBP2A2 prototype. Zero position is the one at room temperature.

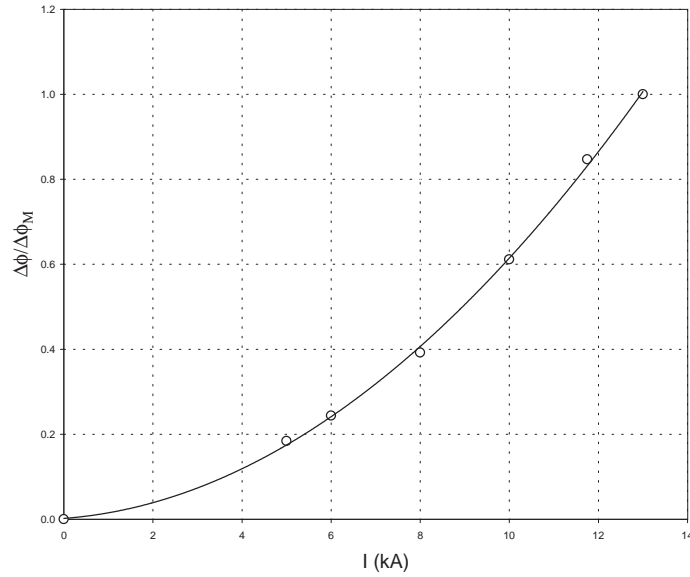


Figure 13: Diameter variation as a function of the exciting current, measured on one side of the prototype MBP2O1. Variations are normalized to their maximum value  $\Delta\phi_M$  at 13.4 kA.

$7 \cdot 10^6$  J is stored in the magnet. When a quench happens, part of such an energy is dissipated by Joule effect in the cable and the magnet warms up. The temperature in the cable can easily increase up to 300 degrees and that leads to an increase of the temperature of the whole cold mass, which depends on the magnet protection and rises in general up to around 30 K [12].

With our optical system, we could measure displacements of the dipole end centre due to the quench-induced warm up of the cold mass. An example, concerning a provoked quench at the nominal current is given in figure 14. Due to the limited bandwidth of our system, it is impossible to observe the fast transient at the very beginning of the quench.

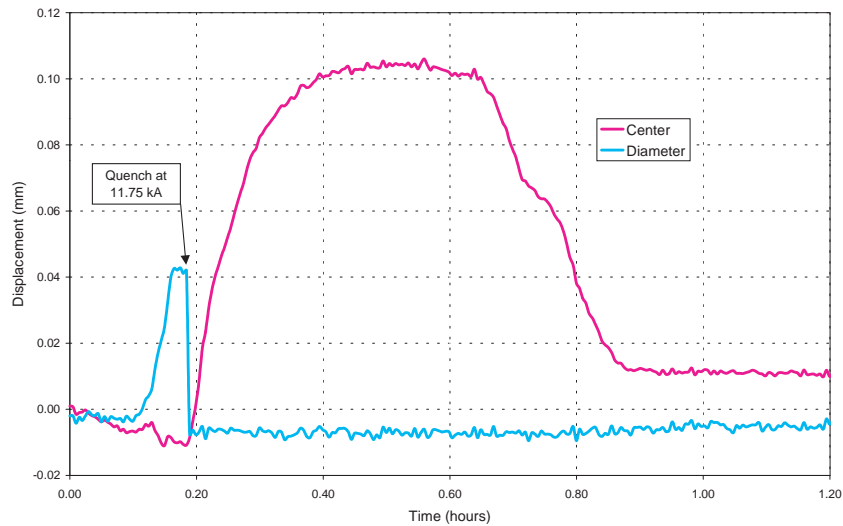


Figure 14: Displacement of one end of the prototype MBP2O1 after a provoked quench at 11.75 kA.

After the quench, the centre cold mass end starts moving and it slowly recovers its

original position, while the refrigeration system absorbs the released energy and recovers the operational temperature of 1.9 K. The temperature increase of the cold mass depends both on the current flowing in the cables and on the parameters of the quench protection system. By analysing quenches at different currents, leading to different temperatures, we found that the original centre position is recovered within few micrometers, with typical time constants from 20 to 50 minutes, which depend on the maximum temperature increase and on the efficiency of the refrigerating system.

Notice that the cold mass diameter, which increases because of the electromagnetic forces, suddenly recovers its original value after the quench (within few micrometers) and it is almost not affected by the magnet warm up: actually, we are in a temperature range (from 1.9 to about 30 K) where the material dilatation is not relevant.

## 5 Conclusions

We described the principle, the constructive details and the first results of a novel device intended to measure transverse displacements between the cold mass and the cryostat of an LHC dipole. The device is fully operational in all the required conditions, i.e., at room temperature and pressure, during transportation and at 1.9 K in vacuum at the dipole operational conditions.

The sensitivity and the precision of the measured displacements is fully satisfactory for the needs of the LHC project, i.e. displacements of the order of magnitude of a few 0.01 mm can be easily detected.

The band-width of our device is rather limited, thus one can detect displacements in a quasi-steady-state situation. Indeed this allowed us to observe with high precision displacements during thermal transient of several hours.

The long term exploitation of this device in a test cell-lattice of LHC will eventually provide us useful information on the fine alignment of the LHC dipoles in operational conditions.

## Acknowledgements

We would like to acknowledge G. Ballerini, R. Délez and M. Rossi for helping in the design and construction of the optical heads, G. Patti and N. Mermillod for the mechanical conception and installation, and S. Aznar Badillo, M. Bajko, S. Goy Lopez and P. Guillieron for the help in the installation and the alignment of mirrors and optical heads. We wish also to thank C. Wyss for his support to our work and for the useful discussions we had with him. We finally thank G. Morpurgo and the CERN groups LHC-CRI and LHC-MTA (in particular M. Buzio and P. Pugnât from LHC-MTA) for their support during the data acquisition.

## References

- [1] *The Large Hadron Collider, CERN Yellow Report 95-05* (1995)
- [2] Bartolini R and Scandale W 1997 *CERN LHC-MMS Internal Note 97-12*
- [3] Inaudi D *et al* 1994 *Sensors and Actuators A* **44** 125-30
- [4] Inaudi D 1995 *Optical Engineering* **34** 1912-5
- [5] Inaudi D *et al* 1996 *SPIE* **2718** 251-57
- [6] Glisic B *et al* 1999 *SPIE* **3670** 505-513
- [7] Inaudi D *et al* 1999 *SPIE* **3587** 50-59
- [8] Inaudi D 1997 *Fibre Optic Sensor Network for the Monitoring of Civil Structures*, (Lausanne, CH: *EPFL Ph.D. Thesis 1612*)

- [9] Glisic B 2000 *Fibre Optic Sensor and Behaviour in Concrete at Early Age*, (Lausanne, CH: *EPFL Ph.D. Thesis* **2186**)
- [10] Fakra S 1999 *Deformation measurements on the LHC-CERN cryodipole: a SOFO sensor prototype*, *IMAC-EPFL Research Report* (Lausanne, CH)
- [11] Redaelli S 2000 *Studio e analisi delle perturbazioni di campo magnetico nei dipoli e quadrupoli del Large Hadron Collider (LHC)*, *Università degli Studi - Master Degree Thesis* (Milano, I)
- [12] Rodriguez-Mateos F *et al* 2000 *7<sup>th</sup> European Particle Accelerator Conference* 2154-6, also in *CERN LHC Project Report* **418**